A Technique for Characterizing Surfactants on the Air–Sea Interface

JIN WU AND YI WEI

Air–Sea Interaction Laboratory, College of Marine Studies, University of Delaware, Lewes, Delaware

(Manuscript received 27 March 1989, in final form 22 August 1989)

ABSTRACT

An optical-electronic technique has been developed for simultaneous, remote measurements of the surface tension and wave attenuation over the water surface. The technique has been fully tested in a laboratory tank, and tried in the field. Sample results of measurements are presented to illustrate that the technique is an effective method for studying the surfactants on the air–sea interface.

1. Introduction

Phenomena at the interface between the atmosphere and oceans, greatly influencing transfer processes across the sea surface, have long interested atmospheric scientists and oceanographers (Phillips 1977). Efforts in developing the remote sensing of oceans have brought up a further demand of understanding the interface, as sea-surface sensors have been used in almost all developments (Moore 1985). Winds over the world's oceans, however, are generally light. Recent photographs of the ocean surfaces show probable substantial coverages of natural films under prevailing, light wind conditions (Scully-Power 1986). Studies of surface films and their effects on air–sea interaction have, therefore, attracted an ever-increasing attention lately.

Cox and Munk (1954) performed the first systematic study on the damping of ocean ripples by artificial slicks; they observed sun glitters on both clean and slick-covered sea surfaces. Subsequently, Garrett (1972) discussed properties of surface films and their general effects on air–sea interaction. More recently, many investigations were conducted on the wave damping by artificial films over the sea surface (Hühnerfuss et al. 1981, 1983a; Yermakov et al. 1985; Ermakov et al. 1986). Data from these studies done with wave staffs were analyzed by Wu (1989) to indicate that artificial films are very effective in wave damping at low winds with velocities below 7 m s^{-1}, and for short gravity waves with their lengths in the range between 20 and 380 mm. On the basis of these results and the Bragg-scattering mechanism, Wu further reviewed microwave returns from sea-surface slicks (Hühnerfuss et al. 1978; Hühnerfuss et al. 1981; Johnson and Croswell 1982; Hühnerfuss et al. 1983b). The results were found to be generally consistent with those of direct wave measurements, with the maximum damping occurring at surface-wave lengths of about 50 mm.

In summary, there have been enough studies to demonstrate the presence of natural films over the sea surface. Their effects on the wave damping have been investigated extensively with substituted artificial films. For more advanced studies, we need to conduct measurements with natural films to determine their physical properties, and to evaluate their influence on wave structures. An optical-electronic technique has been developed to measure simultaneously the surface tension of, and the wave-damping rate over, the water surface. Similar systems using this technique have been tested in a laboratory tank and on board a catamaran in the field. They have been shown to be effective for studying surfactants on the air–sea interface.

2. Arrangement

a. Test tank

Laboratory tests were conducted in a stainless steel tank, 1.2 m long and 0.15 m wide; see Fig. 1. The tank was divided into three compartments as shown in the figure; the center compartment with a length of 1.12 m was the test section, with two narrow end compartments serving for overflow purposes. The total depth of the tank was 0.25 m, and the crest of the weirs, which divided the test and overflow sections, were 50 mm below the top of the tank. Both seawater and freshwater were used. Before the experiment, the sample water was introduced into the center compartment through the intake at the bottom of the tank. In order to clean the water surface through overflowing over the weirs, the rate of introduction was greatly reduced when the water level approached the weir crests. Following a sufficient period of overflowing over the weirs, the inflow was stopped and the water level in the test sec-

Corresponding author address: Dr. Jin Wu, Air–Sea Interaction Laboratory, College of Marine Studies, University of Delaware, Lewes, Delaware 19958.

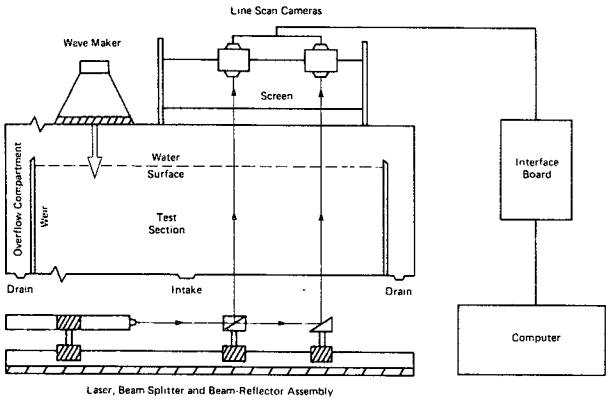

FIG. 1. General arrangement.

tion was dropped, also through the intake, to slightly below the weir crests to commence measurements over the clean surface. For the study of slick surfaces, films were produced through the aging of natural-water samples in the test section of the tank.

b. Wave generation

The capillary waves were generated by an oscillating plunger with a triangular cross section, as shown in Fig. 1. The plunger attached to the core of a speaker was partially submerged; it could be driven by a signal generator to oscillate vertically at desirable frequency and amplitude. The plunger was supported at the middle length of the tank. Both the tank width and water depth are many times greater than the length of capillary waves; thus, effects of side walls and the bottom of the tank on the propagation and attenuation of waves were not expected.

c. Data acquisition

As shown in Fig. 1, a laser was mounted on an optical bench together with a beam splitter and a beam reflector; two parallel vertical beams at prescribed locations could therefore be produced. Each beam was refracted by the wavy water surface to project an image on the horizontal screen. Two line-scan cameras were used, each receiving one beam-trace on the screen. The detector array of the camera has 512 photodiodes. During each scan, the particular photodiode sensing the maximum light intensity was determined and registered. This photodiode then provided the displacement of the projected beam on the screen from its neutral position; the latter corresponds to the zero water-surface slope. An interface board was used to connect two cameras to a computer, on which not only the data were stored, but operations of the cameras were also programmed to control their scanning speed and threshold setting. In summary, the cameras, interface board, and computer were used to record two time series of beam displacements. As discussed later, these time series were then processed, first to obtain the slopes of capillary waves, and subsequently to determine the surface tension and wave-damping rate.

The steps of data acquisition discussed above are summarized in the block diagram shown in Fig. 2; the data processing will be discussed in the following sections.

3. Principle

a. Determination of water-surface slope

As illustrated in Fig. 3a, the water surface has a slope $s = \tan\sigma$, where σ is the angle between the incipient, vertical laser beam and the normal to the disturbed water surface. This angle is the same as that between the tangent to the disturbed water surface and the mean water surface. As the laser beam crosses the water sur-

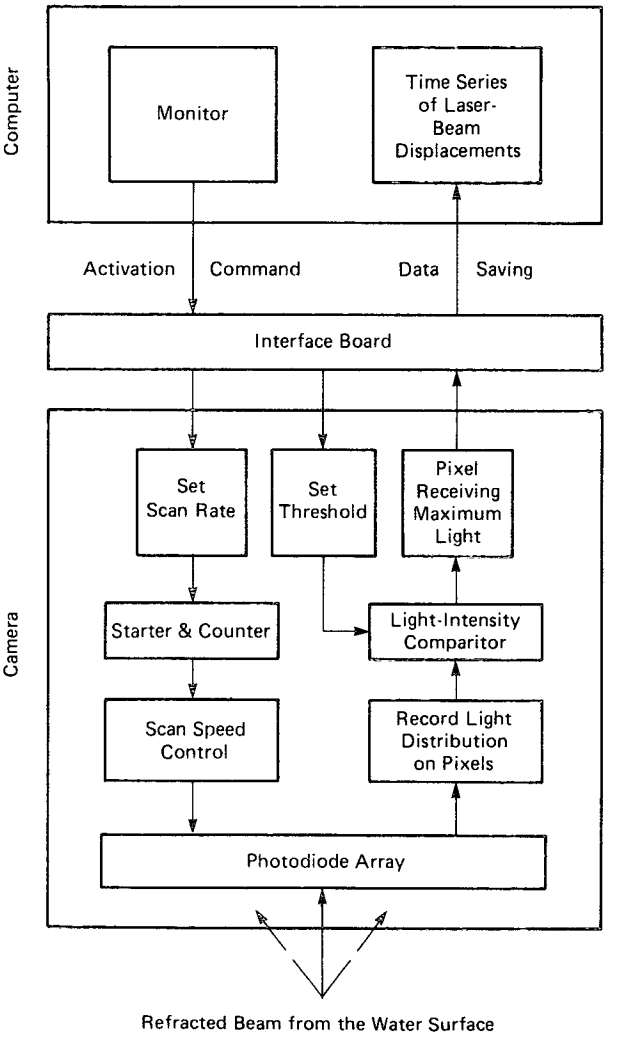

FIG. 2. Block diagram of data acquisition.

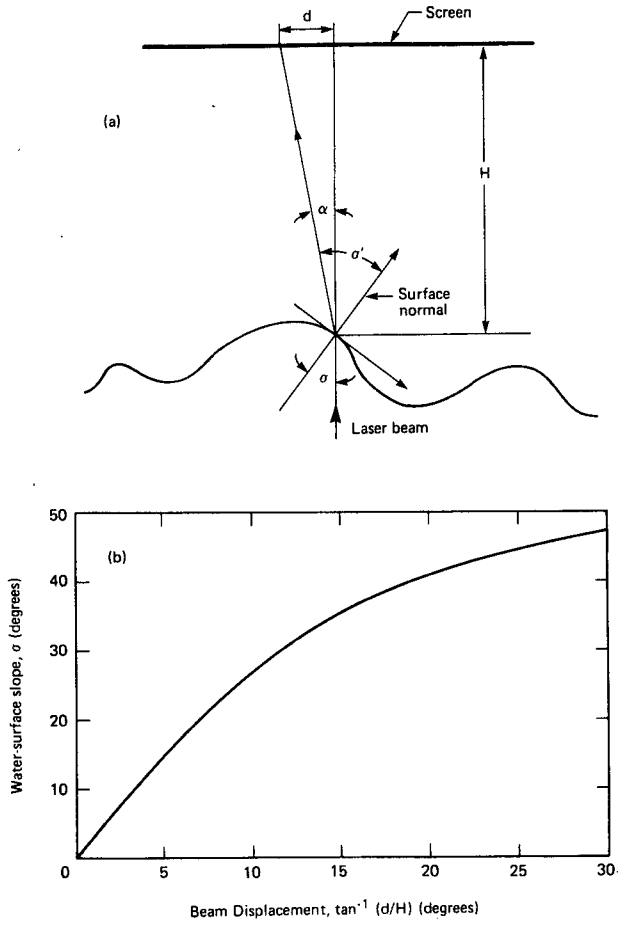

FIG. 3. Measurements of surface slopes: (a) light refraction by a wavy surface and (b) water-surface slopes and beam displacements.

face, it is refracted at an angle σ' from the same normal. Following Snell's law, we have

$$\sin\sigma/\sin\sigma' = n'/n$$

$$(n/n')\csc\alpha - \cot\alpha = \cot\sigma \qquad (1)$$

where n and n' are indices of refraction for water and air, respectively, and α is the difference between σ' and σ. The displacement of the beam, d, on the horizontal screen from its neutral position can be related to the water-surface slope as

$$s = \tan\sigma = 1/[(n/n')\csc\alpha - \cot\alpha],$$

$$\alpha = \tan^{-1}(d/H) \qquad (2)$$

where H is the elevation of the screen above the mean water surface. This elevation was kept at no less than 500 mm, while the height of generated capillary waves was no greater than 1 mm. Any error introduced by the variation of the water-surface elevation on the slope measurement was, therefore, negligible. The relation of the surface slope to the beam displacement is shown in Fig. 3b. With this functional variation, the beam displacements continuously recorded by two cameras can be transferred into the temporal distributions of water-surface slopes; see Fig. 4. The upstream trace in the figure is that recorded by the camera closer to the wave maker; the downstream trace is from the camera farther away from the wave maker. The damping is clearly illustrated by differences in the two traces.

b. Determination of wave parameters

In Fig. 4, Δx is the distance between two beams, which is preset. The water-surface slope recorded are generally sinusoidal, as only small-amplitude waves were generated to avoid the hydrodynamic instability. The period of two slope traces are identical; it is also the same as that of the wave maker. The time lag between the traces, Δt as shown in Fig. 4, can be easily determined. The phase velocity of capillary waves, c, can thus be obtained from

$$c = \Delta x/\Delta t \qquad (3)$$

in which x is the horizontal distance from the wave maker, and t is the time. The length of generated capillary waves was subsequently obtained from $\lambda = 2\pi c/$

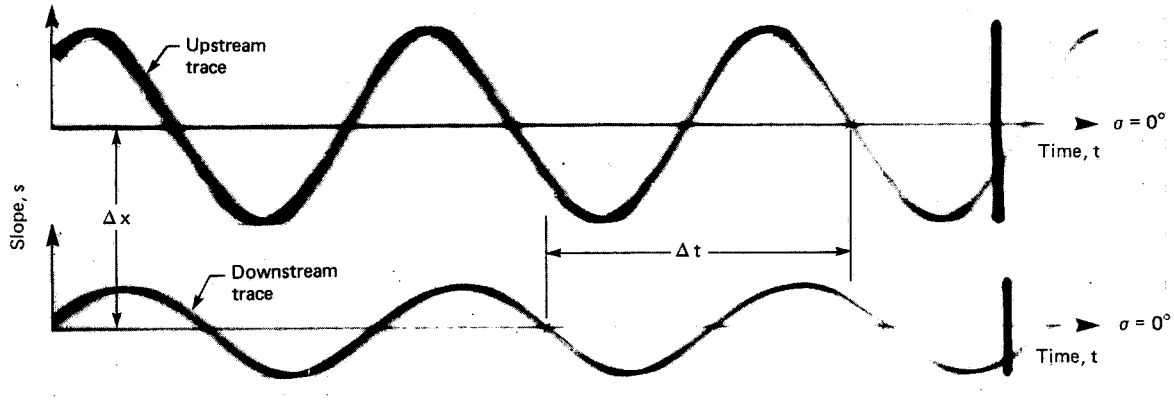

FIG. 4. Sample traces and determinations of phase velocity, length and profile of capillary waves.

ω, where ω is the radian frequency of waves. The latter, as discussed earlier, was also preset.

Following the determination of phase velocity, the temporal distribution of the water-surface slope, $s(t)$, was transferred to the spatial variation of the water-surface slope, $s(x)$, through the transformation $dx = c\,dt$. The local height of capillary waves, h_i, was then obtained from the slope profile through the following integration,

$$h_i = \int_{x_i}^{x_i+\lambda/2} s(x)dx, \quad s(x_i) = s(x_i + \lambda/2) = 0,$$
$$i = 1, 2, \cdots, n \quad (4)$$

where n is the number of waves in a record; x_i indicates the location of the wave troughs or crests, where $s(x_i) = 0$. The wave troughs and crests were located on the computer by finding the zero water-surface slope. The mean wave height was calculated from $\bar{h} = \sum_{i=1}^{n} h_i/n$, and was then taken as the measured wave height.

4. Measurements

a. *Propagation and attenuation of capillary waves*

Taking into account both gravity and surface-tension effects, the dispersion relationship for surface waves in deep water, in terms of frequency, is (Lamb 1932)

$$\omega^2 = (g + Tk^2/\rho)k \quad (5)$$

where k is the wavenumber, g is the gravitational acceleration, T is the surface tension, and ρ is the density of water. This relationship has been verified in a number of experiments.

The energy decay of simple progressive waves can be expressed as (Lamb 1932)

$$E = E_0 \exp(-4\nu k^2/c_g X) \quad (6)$$

where E_0 and E are the energies of waves at different distances from the wave maker, x_0 and $x_0 + X$, respectively; ν is the kinematic viscosity of water; and c_g is the group velocity of waves. The wave energy and group velocity can be obtained, respectively, from

$$E = \rho g h^2/8 \quad (7)$$

$$c_g = \frac{1}{2}(g + 3Tk^2/\rho)(gk + Tk^3/\rho)^{-1/2}. \quad (8)$$

With the presence of surface films, there is an additional damping, but the energy decay still follows an exponential trend (Davies and Vose 1965),

$$E = E_0 \exp(-\beta x) \quad (9)$$

where β includes the damping due to both viscosity and surface film.

b. *Measurements of surface tension and wave damping*

The dispersion relationship shown in Eq. (5) can be rewritten for the purpose of determining the surface tension as

$$T = \rho\lambda(c^2 - g\lambda/2\pi)/2\pi \quad (10)$$

of which the quantities on the right-hand side are either known or measured as described in the last section. The key measurement is, of course, the phase velocity, from which the wavelength is also determined.

From the measured wave height, the local wave energy could be obtained from Eq. (7). Compiling the energies determined at different distances, the damping coefficient defined in Eq. (9) could be determined. During the study, measurements of wave damping over both clean and slick-covered surfaces were separately performed. The additional damping due to surfactants could, therefore, be obtained from the difference in dampings measured from two surfaces.

5. Results

a. *Laboratory test*

Extensive experiments have been conducted with this system in the laboratory. Both freshwater and seawater samples were used.

1) SURFACE TENSION

In addition to the measurements with the optical-electronic technique, the surface tension in the test compartment was also determined with a Wilhelmy surface tensiometer (Adamson 1982), of which the tensile force from the water surface acting on a thin blade, 25 mm wide, was measured with a precision balance at the instant when the blade was lifted to be detached from the water surface. The measurements with these two techniques are compared in Fig. 5; the

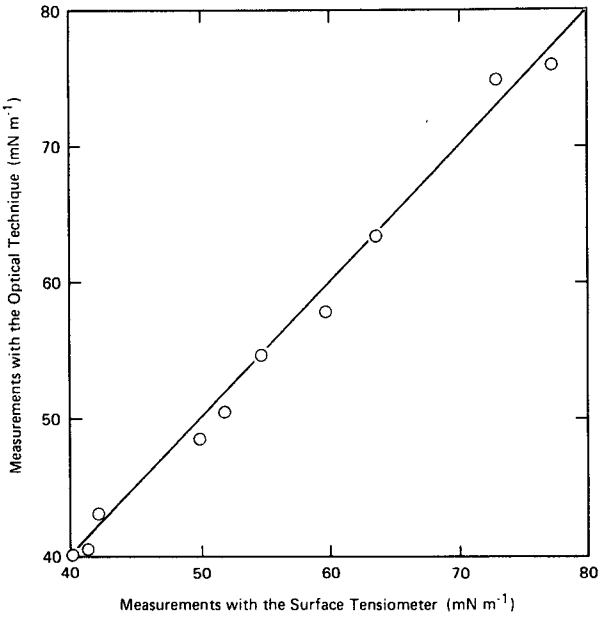

FIG. 5. Comparison of surface tensions measured with optical technique and with surface tensiometer.

two sets of results are seen to be consistent. The repetitiveness of optical measurements, however, was much better than that of surface-tensiometer measurements. This is perhaps due to the fact that the optical technique has a much higher resolution.

2) WAVE DAMPING

As described earlier, the heights of waves were obtained at various distances from their generator; the results are presented in Fig. 6. The measured wave heights are seen in the figure to follow well the exponential decay curves, illustrated by solid lines fitted to the data. The surface film is shown to have substantial effects on the wave attenuation. The slope of lines corresponding to the damping coefficient β in Eq. (9) can be determined. The surface tension and damping rate measured with the present technique are consistent with those reported previously, such as Lucassen's (1981) results on the relationship between the wave dumping and the surface dilational modules. Here, we are more interested in demonstrating the feasibility of studying surfactants with this technique.

b. Field deployment

As discussed earlier, in situ measurements of natural film over the sea surface are necessary in quantifying their properties as well as their efficiency on the wave damping. Furthermore, the natural slick is generally finite in size. Its physical properties and wave-damping effects vary with the wind fetch from the leading edge of the slick. A rather sudden change of the surface roughness from the clean to slick-covered surface also induces the development of an internal boundary layer (Bradley 1968). The wind stress along with wave and current properties are, therefore, all modified. Moreover, surface waves could modulate film properties along their profile to introduce zones of convergence and divergence. In summary, for a more meaningful

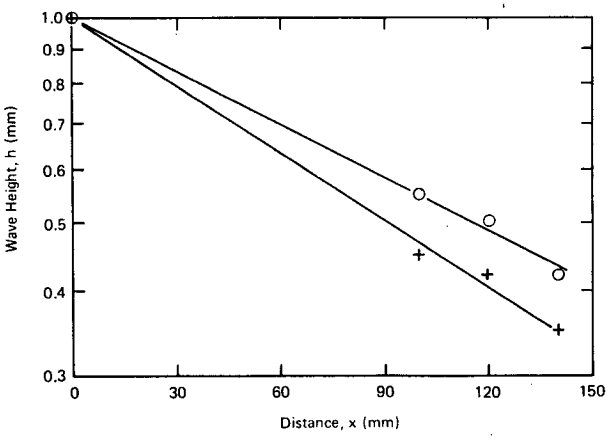

FIG. 6. Spatial wave damping under different surface tensions of 69 mN m^{-1}, O; and 59 mN m^{-1}, +.

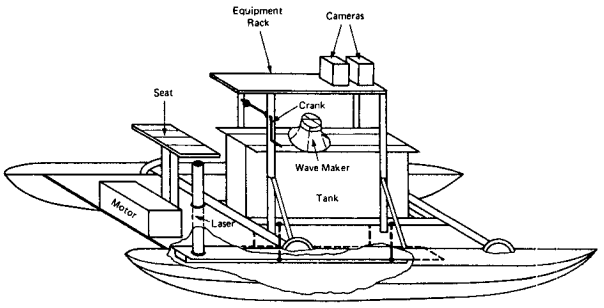

FIG. 7. Instrumented catamaran for in-situ measurements of surfactants.

study of surfactants and their effects, we need to measure not only in situ the surface properties but also the variations of highly localized film properties, and then match these variations with those of wind, waves, and currents.

In order to perform in situ measurements, our laboratory-tested system was modified and placed on a mobile catamaran; see Fig. 7. It could be either launched from shore or deployed from a research vessel. The catamaran was powered with an outboard motor; it could, therefore, transect the slick to measure the spatial variation of film properties and its effects. When the catamaran reached its designated station, the motor was stopped and taken out of the water before measurements to avoid any possible disturbance or contamination. A tank having identical dimensions as that used in the laboratory, but without the overflow compartments, was mounted on the catamaran. The tank was bottomless and could be lowered into the sea to capture a portion of the sea surface in order to perform similar measurements as we did in laboratory. Since the tank is much shorter than the length of dominant ocean waves, films over various portions of the dominant-wave profile could be captured. As shown in Fig. 7, the optical components consisting of beam-splitter and beam-reflector assembly were placed in a water-tight compartment below the tank, and the laser was mounted inside a vertical tube above the deck. Mirrors were used inside the tube and the compartment to guide the laser beam. The wave maker and cameras were the same as those used in the laboratory. A portable computer was used for the data acquisition. An onboard power generator was used to supply power to all electrical components.

Motions of the catamaran, principally pitch and roll, obviously make the measurements difficult in the field. The cross-tank disturbances could make the light beams stray away from the arrays of the line-scan cameras, resulting in a loss of signals. The longitudinal disturbances could add noise to the signals produced by capillary waves. Two measures were taken to deal with these problems. A cylindrical lens was placed in front of the cameras to focus the laterally strayed beams

onto the arrays of the line-scan cameras. To recover the signal from the noise-contaminated data, Fourier analyses of the data were performed to determine their spectra. The phase difference between two trains of capillary waves was then obtained from the phase difference of their spectra. This practice is generally used in the data processing when the frequency of signals is known. Furthermore, the damping rate could be calculated from the magnitude of the spectral components. We have conducted preliminary tests in the field, and the results are encouraging.

It was suggested that the film could attach to the sides of the tank when it was lowered into the water. A washdown pump was, therefore, installed to clean both internal and external sides of the tank when it is lifted out of the water. Additional laboratory measurements will be conducted with natural film to futher evaluate these effects and our cleaning technique.

6. Concluding remarks

Simultaneous measurements of the surface tension and damping rate using the same dataset is the most unique feature of our technique. We have already used this technique to study successfully a series of phenomena associated with surfactants. These include the production of film through aging, the determination of surface dilational modulus, and the damping of waves of various frequencies over different surfaces. The other important feature of our technique is that it is designed to be used in both the laboratory and the field.

Acknowledgments. The authors are very grateful for valuable help provided by Mr. Sterling Tebay in the hardware development and by Dr. Dennis Trizna in the data analysis. The sponsorship of their work was provided by the Ocean Chemistry Program, Office of Naval Research under Contract N00014-86-K-0614.

REFERENCES

Adamson, A. W., 1982: *Physical Chemistry of Surface.* John Wiley & Sons, New York.

Bradley, E. F., 1968: A micrometeorological study of velocity profiles and surface drag in the region modified by a change in surface roughness. *Quart. J. Roy. Meteor. Soc.,* **94,** 361–379.

Cox, C. S., and W. H. Munk, 1954: Statistics of the sea surface derived from sun glitter. *J. Mar. Res.,* **13,** 198–227.

Davies, J. T., and R. W. Vose, 1965: On the damping of capillary waves by surface film. *Proc. Roy. Soc. London,* **A286,** 218–234.

Ermakov, S. A., A. M. Zujkova, A. R. Panchenko, S. G. Salashin, T. G. Talipova and V. I. Titov, 1986: Surface film effect on short wind waves. *Dynamics Atmos. Oceans,* **10,** 31–50.

Garrett, W. D., 1972: Impact of natural and man-made surface films on the properties of the air–sea interface. *The changing chemistry of the Oceans,* Almquist and Wiksell, Stockholm.

Hühnerfuss, H., W. Alpers, W. D. Garrett, P. A. Lange and S. Stolte, 1983a: Attenuation of capillary and gravity waves at sea by monomolecular organic surface films. *J. Geophys. Res.,* **88,** 9809–9816.

——, ——, A. Cross, W. D. Garrett, W. C. Keller, P. A. Lange, W. T. Plant, F. Schlude and D. L. Schuley, 1983b: The modification of *X* and *L* band radar signals by monomolecular sea slicks. *J. Geophys. Res.,* **88,** 9817–9822.

——, —— and W. L. Jones, 1978: Measurements at 13.9 GHz of the radar backscattering cross section of the North Sea covered with an artificial surface film. *Radio Sci.,* **13,** 979–983.

——, ——, ——, P. A. Lange and K. Richter, 1981: The damping of ocean surface waves by a monomolecular film measured by wave staffs and microwave radars. *J. Geophys. Res.,* **86,** 429–438.

Johnson, J. W., and W. F. Croswell, 1982: Characteristics of 13.9 GHz radar scattering from oil films on the sea surface. *Radio Sci.,* **17,** 611–617.

Lucassen, J., 1981: Effect of surface-active material on the damping of gravity waves: A reappraisal. *J. Colloid Interface Sci.,* **85,** 52–58.

Lamb, H., 1932: *Hydrodynamics.* 6th ed., Cambridge University Press, Cambridge.

Moore, R. K., 1985: Radar sensing of the ocean. *I.E.E.E. J. Oceanic Eng.,* **QE-10,** 84–112.

Phillips, O. M., 1977: *The Dynamics of the Upper Ocean.* 2nd ed., Cambridge University Press.

Schully-Power, P., 1986: Navy oceanographic shuttle observations—Mission report, STS 41-G. Navy Underwater System Center, Newport, Rhode Island.

Wu, Jin, 1989: Suppression of ripples by surfactant—Spectral effects deduced from sun-glitter, wave-staff and microwave measurements. *J. Phys. Oceanogr.,* **19,** 238–245.

Yermakov, S. A., A. R. Panchenko and T. G. Talipova, 1985: Damping of high-frequency wind waves by artificial surfactant films. *Izv. Atmos. Oceanic Phys.,* **21,** 54–58.